



Electrochemical investigations and characterization of a metal hydride alloy ($\text{MmNi}_{3.6}\text{Al}_{0.4}\text{Co}_{0.7}\text{Mn}_{0.3}$) for nickel metal hydride batteries

S. Nathira Begum*, V.S. Muralidharan, C. Ahmed Basha

Central Electrochemical Research Institute, Karaikudi 630006, India

Received 27 October 2007; received in revised form 5 December 2007; accepted 12 December 2007

Available online 3 January 2008

Abstract

The use of new hydrogen absorbing alloys as negative electrodes in rechargeable batteries has allowed the consideration of nickel/metal hydride (Ni/MH) batteries to replace the conventional nickel cadmium alkaline or lead acid batteries. In this study the performance of trisubstituted hydrogen storage alloy ($\text{MmNi}_{3.6}\text{Al}_{0.4}\text{Co}_{0.7}\text{Mn}_{0.3}$) electrodes used as anodes in Ni/MH secondary batteries were evaluated. MH electrodes were prepared and the electrochemical utilization of the active material was investigated. Cyclic voltammetric technique was used to analyze the beneficial effect of the alloy by various substitutions. The electrochemical impedance spectroscopic measurements of the Ni/MH battery were made at various states of depth of discharge. The effect of temperature on specific capacity is studied and specific capacity as a function of discharge current density was also studied and the results were analyzed. The alloy metal hydride electrode was subjected to charge/discharge cycle for more than 200 cycles. The discharge capacities of the alloy remains at 250 mAh/g with a nominal fading in capacity (to the extent of ~ 20 mAh/g) on prolonged cycling. © 2007 Elsevier B.V. All rights reserved.

Keywords: Rare earth alloys and compounds; Energy storage materials; Metal hydrides; Transition metal alloys and compounds; Electrochemical reactions; Electrochemical impedance spectroscopy

1. Introduction

The world wide market for rechargeable batteries for consumer electronic applications is growing at a record pace due to increased end user demand for portable devices such as cellular phones, lap-top computers, camcorders and other electronic devices. There is also an increasing demand for compact, lighter batteries with high capacity for use in smaller/lighter electrical and electronic applications. Until recently, nickel/cadmium (Ni/Cd) batteries were meeting these requirements. Nickel/metal hydride (Ni/MH) batteries using hydrogen storage alloy as negative electrode material represent the fastest growing segment of this rechargeable battery market for one to one replacement in electronic devices due to their higher energy density (both in terms of weight and volume) and good cycle life. These batteries have more environmentally acceptable chemistry than to Ni/Cd batteries, owing to the absence of such hazardous materials like

Pb, Cd and Hg [1–4]. It is also becoming more competitive with lithium ion battery in terms of volumetric energy density, long life, and inherent protection against over charge/discharge. Ni/MH battery has high rate charge/discharge capability and good voltage match with Ni/Cd and Zn/MnO₂ batteries. It has low internal impedance required especially in the applications such as wireless mobile communications where such parameters are critical. Ni/MH sealed cells are easily constructed to consume effectively the oxygen and hydrogen gas evolved during over charge/discharge, allowing prismatic design with superior packaging and heat management capabilities. The major difference of Ni/MH from Ni/Cd battery is the use of hydrogen storage alloy as the negative active material which is capable of undergoing a reversible hydrogen absorbing–desorbing reaction when the battery is charged and discharged. The interactions between hydrogen and metals have been extensively investigated from both fundamental and practical view points [5]. Conventional hydrogen/metal oxide cells use hydrogen gas stored in pressure cylinders. The application of hydrides replaces gaseous hydrogen storage with metal hydride, with hydrogen produced by the following reaction:

* Corresponding author. Tel.: +91 4565 227550; fax: +91 4565 227713.
E-mail address: nava_572004@yahoo.co.in (S.N. Begum).



where M is the intermetallic compound or alloy capable of reversibly absorbing hydrogen. The hydrogen absorbing alloys used in secondary batteries require essential features like high hydrogen absorption capacity and superior corrosion resistance in alkaline environment. Libowitz demonstrated reversible hydrogen absorption and desorption in ZrNiH_3 [6]. Investigations on Ni_2Ti based and LaNi_5 based alloys were found to have limited life cycle which is too poor to be useful in practical batteries [7–11]. Percheron Guegan et al. [8,12] were first to recognize the correlation between the gaseous pressure composition isotherm and the electrochemical properties of LaNi_5 based alloy. They suggested that the long-term stability of LaNi_5 electrodes could be improved by partly replacing La and Ni by other alloying elements. Binary LaNi_5 suffers from severe corrosion during cycling due to intermetallic decomposition and pulverization in the alkaline electrolyte, resulting in a fast decrease of the capacity as a function of cycle number [11,13–15]. The use of misch metal (Mm, a mixture of rare earth metals 51% La, 23% Ce, 23% Nd, and 3% Pr) and transition metals, (M) as components of the matrix of kind $\text{MmLa}_{1-x}(\text{NiM})_5$ in hydrogen absorbing alloys were investigated [16–20]. It was noted that a misch metal (Mm) predominantly based on La (>50 wt%) and the use of Ni-substituting elements (M) like Co, Al and Mn greatly improve the intrinsic characteristics of the alloys for absorbing hydrogen electrochemically. This would enhance cycle life-time, high discharge capability, thermal stability and specific capacity which are the main performance characteristics of the rechargeable battery. Since the MH electrode mainly influences the performance of Ni/MH batteries, research is focused to design and fabricate a suitable negative electrode to fulfill the demands of Ni/MH batteries. With these entire objectives in mind, the stoichiometry of hydrogen absorbing alloy $\text{MmNi}_{3.6}\text{Al}_{0.4}\text{Co}_{0.7}\text{Mn}_{0.3}$ was chosen for investigation from the point of view of its capacity, cycle life, and charge/discharge characteristics. Cyclic voltammetric (CV) studies and electrochemical impedance spectroscopic (EIS) measurements were also made to evaluate the performance of the electrode. The results are reported in the paper.

2. Experimental

A hydrogen storage alloy of nominal composition $\text{MmNi}_{0.36}\text{Al}_{0.4}\text{Co}_{0.7}\text{Mn}_{0.3}$ was obtained from Trieibacher, Austria. The average particle size of alloy was 45 μm . The crystal structure was identified by X-ray diffractogram using X-ray diffractometer (PANalytical make, X'per PRO model, Cu $\text{K}\alpha$ radiation). The alloy powder was used as a negative electrode material. In the experimental cell an over dimensional positive electrode namely $\text{Ni}(\text{OH})_2/\text{NiOOH}$ plate was used as a counter electrode for study. A commercial three-compartment electrochemical cell was used for all these experiments. The negative electrode was placed in the central compartment and two $\text{Ni}(\text{OH})_2/\text{NiOOH}$ electrode were placed on either side. The electrolyte in the cell was a 31% analar grade KOH aqueous solution. Triple distilled water was used for solution preparations. Hg/HgO electrode was used as a reference electrode. The MH test electrodes were prepared by mixing the alloy powder (85 wt%), graphite powder (8–10 wt%) and poly tetra fluoro ethylene (PTFE) suspension (3–5 wt%). The resulting mixture was then pasted over either side of a current collector made of pure nickel foam (INCO-nickel) and pressed at an optimum pressure of 1000 kg/cm^2 for 10–15 min. The pressed

electrodes were heated to 120–150 °C in a reducing atmosphere for 30 min. The physical thickness of the finished electrodes was about 1 mm. The metal hydride electrodes were inserted into pockets made out of celgard separator cloth (Hoechst Celanese Corporation, USA). The mixing of the active material with the high surface area carbon powder prior to pressing minimizes the electronic resistance as well as increases the mechanical integrity of the electrode. The test electrodes were activated for hydride formation by continuous galvanostatic cycling, until a constant value of the hydrogen capacity was obtained. The activation gives an electrochemical exercise (by oxidation–reduction process) to electrode materials. This has the effect of increasing the lattice defects formation, which is essential for maximum electrode performance at both high and low discharge rates and for removal of any impurities and loose particles. The metal hydride electrodes were found to form and achieve their maximum capacity values with in three to five charge/discharge cycles. During the first cycle, the electrodes were charged at the $C/20$ rate and then by at the $C/10$ rate. The electrodes were discharged at $C/5$ rate.

Before conducting the electrochemical experiments, sufficient time (30 min) was allowed for the potential to stabilize. The electrochemical hydrating/dehydrating reaction of alloy (M) can be represented by the redox reaction.



The specific electrochemical storage capacity C , mAh/g, is calculated from the amount of electricity Q , mAh, discharged from the electrode defined per unit weight of the hydride material in the electrode:

$$C = \frac{Q}{W_{\text{HM}}} \quad (3)$$

where W_{HM} is the mass of active material. The charge/discharge and polarization tests of the experimental electrodes and cells were conducted using a LCN Bitrode model 2–10–12 cycle life tester. The charge/discharge was conducted at predetermined temperature ranging from 0 to 65 °C.

Cyclic voltammetry (CV) is a useful electrochemical technique for investigating electrode/electrolyte interface and superficial charge distribution under potentiodynamic conditions farther from equilibrium [21]. The test electrodes prepared as described above are used as working electrode in CV studies. The counter electrode was a platinum sheet and a Hg/HgO electrode was used as reference. A potentiostat/galvanostat BAS-Zahner IM6 impedance analyzer was used for obtaining cyclic voltammograms (CVs). Prior to cyclic voltammetric studies, the electrodes were activated in 31% analar grade KOH aqueous solution. After resting for 30 min, the cyclic voltammograms were obtained at different scan rates ranging from 10 to 100 mV/s. The scan potential varied from –1.1 to 0.2 V versus Hg/HgO.

Electrochemical impedance spectroscopy (EIS) is an effective technique for analyzing the mechanism of internal structure and structural change over cycling of charge and discharge [22–25]. In order to study AC impedance change over the cycle life, the EIS experiments under open circuit conditions were carried out using the same BAS-Zahner IM6 impedance analyzer. AC impedance studies on this alloy electrode with various compositions of addition agents have been studied and reported [26].

3. Results and discussion

Fig. 1 gives the operating principle of a sealed rechargeable Ni/MH cell. As stated earlier, investigations were carried out with a fabricated MH electrode and the results were presented in Figs. 2–6. The experiments were conducted in the assembled Ni/MH cell and their results were represented in Figs. 7–10.

The $\text{Ni}(\text{OH})_2$ at the positive electrode is oxidized to NiOOH on charge and reduced back to $\text{Ni}(\text{OH})_2$ during discharge. During charge, at the MH negative electrode, reduction of water produces atomic, absorbed hydrogen which diffuses into the lattice of the intermetallic alloy to form a metal hydride. A reverse reaction takes place during discharge. Accordingly the electro-

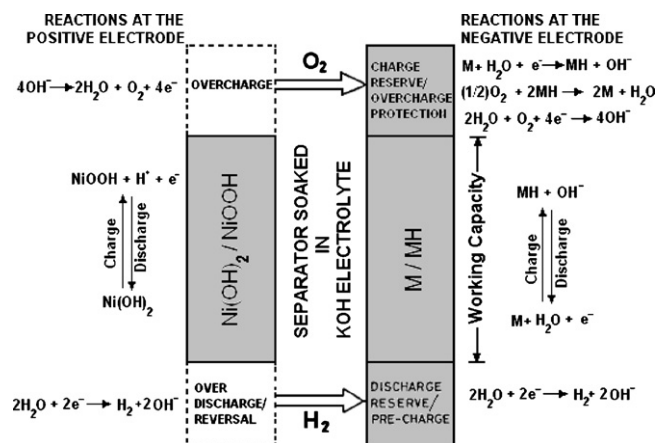


Fig. 1. Operating principle of Ni–MH cell.

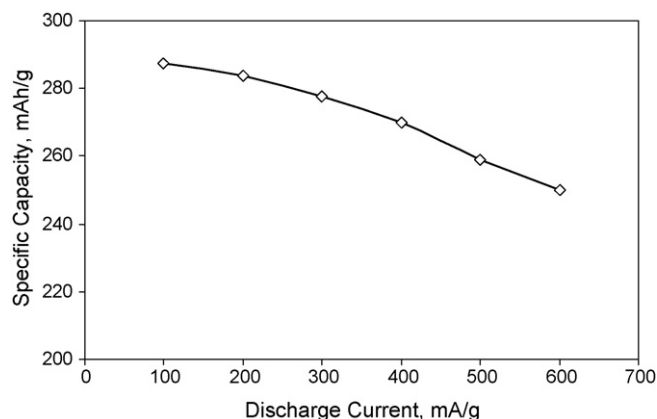


Fig. 4. The variation of specific capacity of the hydrogen storage alloy with discharging current.

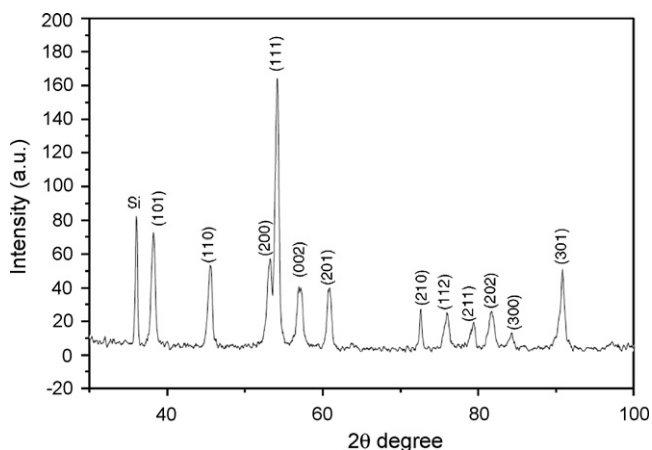


Fig. 2. XRD pattern of the trisubstituted (MmNi_{3.6}Al_{0.4}Co_{0.7}Mn_{0.3}) alloy.

chemical reactions occurring in a Ni/MH cell is represented as follows:

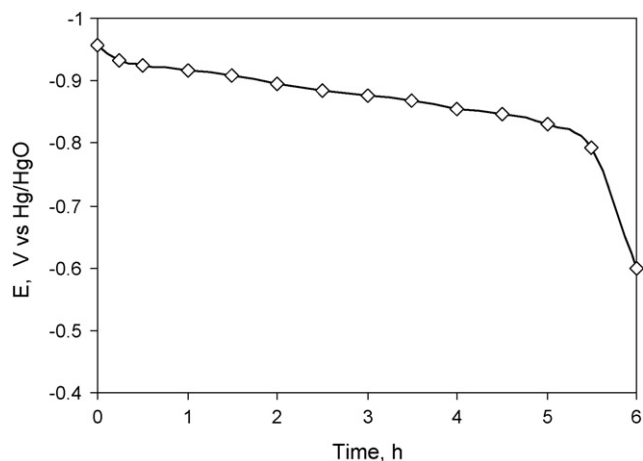
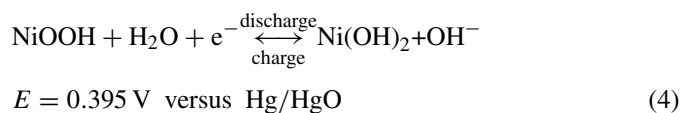
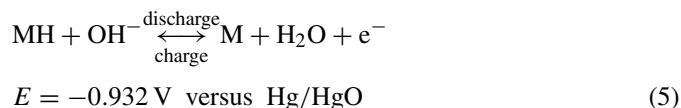


Fig. 3. The variation of discharge voltage with time of the hydrogen storage alloy electrode.

and



accordingly the over all cell reaction is



As a consequence of reactions (4) and (5) there is no net change in the electrolyte quantity or concentration during charge/discharge cycles. Here in Ni/MH batteries the charge–discharge reaction proceeds via homogeneous solid-state mechanism through proton transfer between nickel hydroxide and hydrogen storage alloy, distinguishing it from other batteries such as Ni/Cd, Ni/Fe and Ni/Zn where the electrode reactions proceed through solid-state and/or dissolution–precipitation mechanism. Hence the sources of many performance deficiencies such as change in crystallography change in mechanical integrity, dissolution and recrystallization and reduced electrical conductivity in the oxidized state are eliminated in Ni/MH batteries. This is an

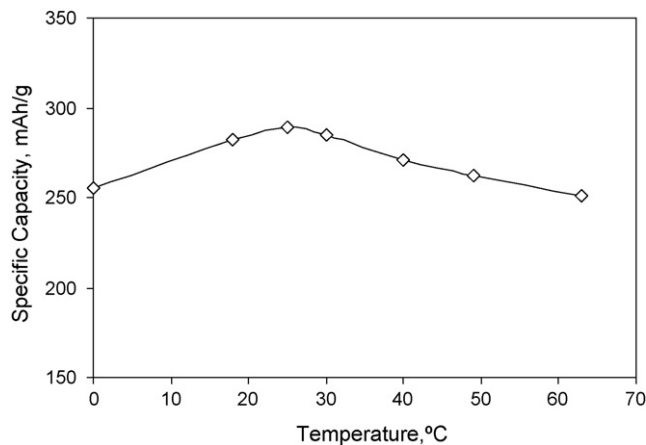


Fig. 5. The variation of specific capacity of the hydrogen storage alloy with temperature.

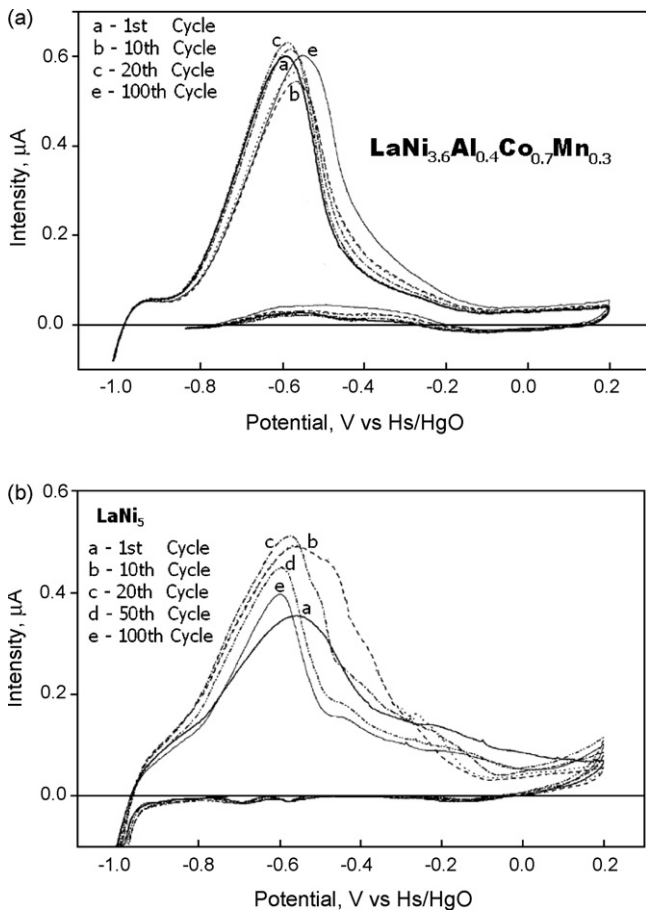


Fig. 6. (a) Cyclic voltammogram of the trisubstituted hydrogen storage alloy (sweep rate = 50 mV/s, $E_{\lambda c} = -1.0$ V, $E_{\lambda a} = 0.2$ V). (b) Cyclic voltammogram of the unsubstituted hydrogen storage alloy (sweep rate = 50 mV/s, $E_{\lambda c} = -1.0$ V, $E_{\lambda a} = 0.2$ V).

attractive feature over Ni/Cd batteries (the electrolyte is concentrated aqueous KOH).

Fig. 2 shows the X-ray diffraction pattern of the alloy. The observed diffraction lines for $MmNi_{0.36}Al_{0.4}Co_{0.7}Mn_{0.3}$ correspond to the JCPDS card no 25–1136. The alloy has AB₅ namely CaCu₅ type hexagonal structure and its lattice parameters a and c are 5.0027 and 4.0558 Å respectively. The unit cell volume is 87.90 Å³

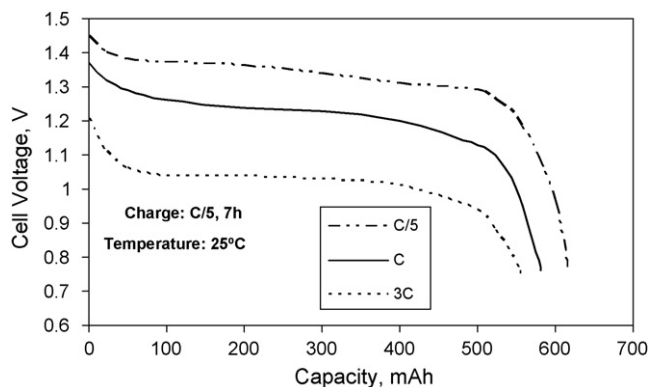


Fig. 7. Effect of discharge rate on the capacity of Ni/MH cell.

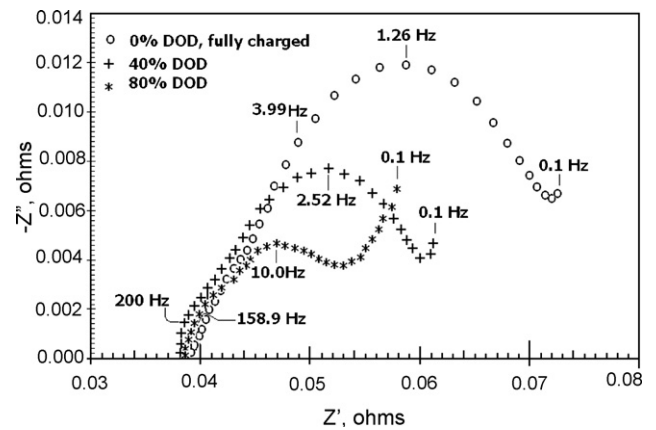


Fig. 8. EIS behavior of the Ni/MH cell at various states depth of discharge (frequency regime 1 kHz to 1 mHz).

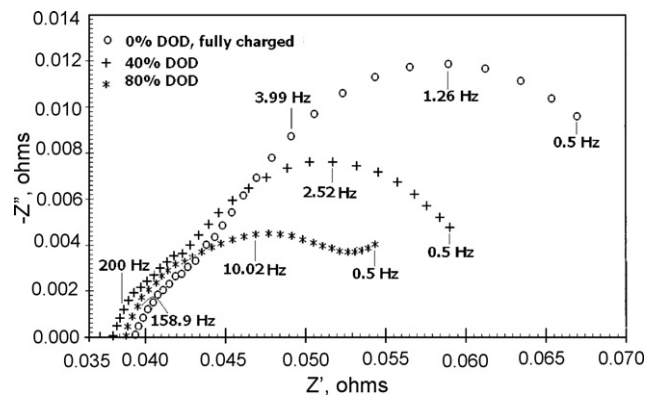


Fig. 9. Expanded Nyquist plots shows two areas on the Ni/MH cell at various states depth of discharge (frequency regime 1 kHz to 0.5 Hz).

A typical constant current discharge curve for the metal hydride electrode is shown in Fig. 3. The metal hydride electrodes were discharged at a constant current of 100 mA/h up to -0.600 V versus Hg/HgO reference electrode. The electrode delivered a total current of 575 mA in 5 h and 45 min (575 mAh).

Fig. 4 shows the specific capacity of the metal hydride alloy electrode at different discharge currents. The specific capacity of the alloy powder at 100 mA, discharge current reaches

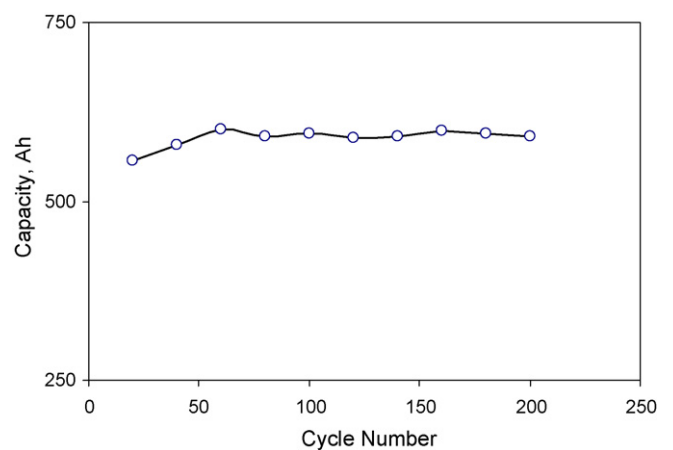


Fig. 10. Life cycle of hydrogen storage alloy electrode (C/5 rate of discharge).

290 mAh/g. At high rate of discharge namely at 600 mA the specific capacity reaches a saturated values of 250 mAh/g. The MH electrode was charged/discharged over 300 cycles. The specific discharge capacity remained at 260 mAh/g at 30 °C.

Fig. 5 shows the specific discharge capacity versus temperature. The discharge capacity was measured at 100 mA/g discharge current. The specific capacity of the MH electrode has a maximum value of 290 mAh/g at 28 °C. The discharged capacity decreased to 250 mAh/g at 0 °C and 245 mAh/g at 65 °C. The electrochemical reaction at the surface of the MH alloy powder is controlled by the charge transfer process at the MH electrode/electrolyte interface and the mass transfer process in the bulk MH alloy. The higher temperature leads to an increase in the charge transfer and mass transfer reactions. However, the higher temperature leads to a decrease in the hydrogen storage capacity in the MH alloy. At high temperatures there is instability of the alloy electrode hence also results in decrease of capacity. At lower temperatures, the reduced desorption rate of the hydrogen increases polarization of alloy electrode causes to decrease the capacity in the MH alloy.

Fig. 6a shows first, tenth, twentieth and hundredth CVs recorded at the scan rate of 50 mV/s for the alloy. From the cyclic voltammograms one observes a shoulder on the water reduction wall and a wide anodic peak located at about –600 mV versus Hg/HgO. About 20 conditioning cycles are necessary for obtaining the stable curve.

Fig. 6b shows the cyclic voltammograms for the unsubstituted LaNi₅ for comparison. From the voltammograms one can note that LaNi₅ the unsubstituted sample shows the more erratic evolution of the curve shape while the trisubstituted sample (MmNi_{3.6}Al_{0.4}Co_{0.7}Mn_{0.3}) shows the smallest change of the curve shape. Thus the partial substitution of Ni by Mn, Al and Co provides stability of the potential and of the peak shape and also brings the intensity stability. So the trisubstituted sample MmNi_{3.6}Al_{0.4}Co_{0.7}Mn_{0.3} shows the smallest change of the curve shape. It has a potential stability as well as the intensity stability.

The discharge rate has an important bearing on the voltage-time curves of Ni/MH cells. Increased rates results in lower cell voltage and decreased capacity. It should be noted that the losses in capacity experienced with Ni/MH cells at high rates are less pronounced than other secondary cells due to the advantage that there is no change in the electrolyte concentration. Fig. 7 shows the discharge performance of Ni/MH cells at various rates (C/5 to 3C). The cells can also be discharged at 5C rate. Due to the endothermic nature of the discharge process, heat evolved during discharge is relatively less than Ni/Cd cells at rates less than C. So Ni/MH cells are more suitable for high discharge rates.

Fig. 8 shows the EIS behavior of Ni/MH cells at various states of charge in the medium frequency regime of 1 kHz to 10 mHz. The well-defined high-frequency charge transfer processes are observed for all the states of charge until the depths of discharge (DOD) exceeds 80% at 5 h rate. The high-frequency intercepts are primarily the resistance of the electrolyte. It is observed that the electrolyte resistance of the Ni/MH cells remains rel-

atively constant during most of the discharge process whereas the interfacial resistance change with the state of charge, which is different from Ni/Cd cells as described else where [27].

Fig. 9 shows the high-frequency response of Fig. 8. Two regions are clearly defined. A typical Nyquist plot for a couple of porous electrodes shows one small arc in the high-frequency domain and one large arc in the low frequency domain. As the cells approach 80% DOD two arcs are overlapped and clear Warburg diffusion impedance is observed.

The life of a battery is ordinarily characterized in terms of the number of charge/discharge cycles that can be delivered or in terms of total life-time in years. It is very difficult to produce general life data in quantitative forms as the life of the battery depends on large number of factors such as discharge rate operating temperature, mechanical stresses, etc. The life cycle performance of the Ni/MH cell was shown in Fig. 10 at C/5 rate of discharge. The capacity of the cell remains almost same even after 200 cycles with out any fading.

4. Conclusion

The application of hydride hydrogen storage and hydride electrode for electrochemical cells shows technological promise. For both the applications the hydride material shows stability in an alkaline environment that contains water and oxygen. The MH alloy powder used for electrode fabrication in this work showed good stability when it was charged and discharged over 200 cycles. The discharge capacity of the alloy electrode, even at high discharge current densities, was found to be more than 250 mAh/g. The high rate discharge capability, the temperature effect on capacity and also life cycle performance of the alloy powder indicated good results. This trisubstituted alloy shows the best results for capacity, discharge rate, wide range of temperature applications and life cycle.

References

- [1] F. Bittner, C.C. Badcock, *J. Electrochem. Soc.* 130 (1983) 193C.
- [2] J.J.G. Willems, K.H.J. Buschow, *J. Less-Common Met.* 129 (1987) 14.
- [3] M. Kanda, M. Yamamoto, K. Kanno, Y. Satoh, H. Hayashida, M. Suzuki, *J. Less-Common Met.* 172–174 (1991) 1227.
- [4] T. Sakai, H. Miyamura, N. Kuriyama, H. Ishikawa, I. Uehara, *Z. Phys. Chem.* 183 (1994) 333.
- [5] H. Oesterreicher, *Appl. Phys.* 24 (1981) 169.
- [6] G. Sansrock, in: P.D. Bennett, T. Sakai (Eds.), *The Electrochemical Society Proceedings Series*, Pennington, NJ, 1994, p. 1.
- [7] G. Bronoel, J. Sarradin, M. Bonnemony, A. Percheron, J.C. Achard, L. Schlapbach, *Int. J. Hydrogen Energy* 1 (1976) 251.
- [8] A. Percheron Guegan, J.C. Achard, J. Sarradin, G. Bronoel, in: A.F. Andresen, A.J. Maeland (Eds.), *Hydride for Energy Storage*, Pergamon, Oxford, 1978, p. 485.
- [9] M.H.J. Van Rijswijk, in: A.F. Andresen, A.J. Maeland (Eds.), *Hydride for Energy Storage*, Pergamon, Oxford, 1978, p. 261.
- [10] T.L. Martin, N.J. Bridger, R. Bennett, R.M. Dell, *Proceedings of the 28th Power Sources Symposium*, Atlantic City, New Jersey, 1978, p. 136.
- [11] J.J.G. Willems, *Philips J. Res.* 39 (Suppliment 1) (1984) 1.
- [12] A. Durairajan, B.S. Haran, R.E. White, B.N. Popov, *J. Power Sources* 87 (2000) 84.
- [13] H. Ye, Y. Huang, J. Chen, H. Zhang, *J. Power Sources* 103 (2002) 293.
- [14] T. Sakai, H. Yoshinaga, H. Miyamura, N. Kuriyama, H. Ishikawa, *J. Alloys Compd.* 180 (1992) 37.

- [15] C.-Y. Seo, S.-J. Choi, J. Choi, C.-N. Park, P.S. Lee, J.-Y. Lee, *J. Alloys Compd.* 350 (2003) 324.
- [16] H. Senoh, K. Morimoto, H. Inoue, C. Iwakura, P.H.L. Notten, *J. Electrochem. Soc.* 147 (2000) 2451.
- [17] G. Zheng, B.N. Popov, R.E. White, *J. Electrochem. Soc.* 143 (1996) 435.
- [18] M. Geng, *J. Alloys Compd.* 217 (1995) 90.
- [19] X. Wang, B. Liu, J. Yan, H. Yuan, D. Song, Y. Zhang, *J. Alloys Compd.* 293–295 (1999) 788.
- [20] T. Sakai, K. Oguro, H. Miyamura, N. Kuriyama, A. Kato, H. Ishikawa, *J. Less-Common Met.* 161 (1990) 193.
- [21] H.S. Kim, M. Nishizawa, I. Uchida, *Electrochim. Acta.* 45 (1999) 483.
- [22] A. Lasia, in: B.E. Conway, J.O'M. Bockris, R.E. White (Eds.), *Modern Aspects of Electrochemistry*, Vol. 35, Academic Plenum Publishers: Kluwer, Dordrecht, New York, 2001.
- [23] S.E. Johnsen, G. Lindbergh, A. Lundqvist, R. Tunold, *J. Electrochem. Soc.* 150 (2003) A629.
- [24] A.M. Svensson, L.O. Valzen, R. Tunold, *Electrochim. Acta* 50 (2005) 2647.
- [25] V. Subramanian, V. Boovaragavan, K. Potukuchi, V. Diwakar, A. Guduru, *Electrochem. Solid-State Lett.* 10 (2) (2007) A25.
- [26] S. Nathira Begum, K. Manimaran, N.G. Ranganathan, M. Ragavan, *Trans. SAEST* 38 (2) (2003) 89.
- [27] C.D.S. Tuck, in: C.D.S. Tuck (Ed.), *Modern Battery Technology*, Ellis Horwood Limited, West Sussex, England, 1991, p. 60.